Scientific Research

Capacitive Properties of Mesoporous Mn-Co Oxide Derived from a Mixed Oxalate

Yong Yan, Bingcai Wu, Cuihong Zheng, Daolai Fang[*]

School of Materials Science and Engineering and Anhui Key Laboratory of Metal Materials and Processing, Anhui University of Technology, Ma'anshan, China.
Email: [*]fangdl@ahut.edu.cn

ABSTRACT

A mesoporous Mn-Co oxide for supercapacitors was derived from a mixed oxalate $Mn_{0.8}Co_{0.2}C_2O_4 \cdot nH_2O$, which was synthesized by a solid-state coordination reaction at room temperature. The synthesized mixed Mn-Co oxalate was decomposed in air at 250°C, resulting in a tetragonal spinel Mn-Co oxide with a primary particle size less than 100 nm. The obtained Mn-Co oxide presents a mesoporous texture with a specific surface area of 120 $m^2 \cdot g^{-1}$. Electrochemical properties of the Mn-Co oxide electrode were investigated by cyclic voltammetry and galvanostatic charge/discharge in 6 $mol \cdot L^{-1}$ KOH electrolyte. The Mn-Co oxide electrode delivered specific capacitances of 383 and 225 $F \cdot g^{-1}$ at scan rates of 2 and 50 $mV \cdot s^{-1}$, respectively. Subjected to 500 cycles at a current density of 1.34 $A \cdot g^{-1}$, the symmetrical Mn-Co oxide capacitor showed specific capacitance of 179 $F \cdot g^{-1}$, still retaining ~85% of its initial capacitance. The obtained Mn-Co oxide material showed good capacitive performance, which was promising for supercapacitor applications.

Keywords: Supercapacitors; Manganese Oxide; Solid-State Reaction; Cyclic Voltammetry; Capacitive Performance

1. Introduction

Electrochemical supercapacitors possess the unique energy-storage performance, such as greater power density and longer cycle life than secondary batteries, as well as higher energy density than conventional capacitors [1], showing great potential to be used in the areas of hybrid power sources, peak power sources, backup power storage, lightweight electronic fuses, starting power of fuel cells [2,3]. Generally the supercapacitors can be classified into two categories: electrical-double-layer capacitors (EDLCs), which build up electrical charge at the electrode/electrolyte interface [4,5], and pseudocapacitors, which are based on reversible faradic redox reactions at the interfaces at certain potentials [6-10].

Recently, with the purpose of achieving high energy density supercapacitors, great efforts have been devoted to search for excellent pseudocapacitive materials [11-20]. Amorphous hydrated ruthenium oxide has been demonstrated to be an excellent pseudocapacitor material, which exhibits a high conductivity, good electrochemical stability, and a large specific capacitance (SC) of 720 - 760 $F \cdot g^{-1}$ [21]. However, high cost and toxicity of the ruthenium oxide greatly limit its commercial applications. Thus, other less expensive and less toxic transition metal

oxides, such as amorphous and crystallized MnO_2 [11-14], nanostructured NiO [15,16], and mesoporous and nanowire-array Co_3O_4 [17,18], have been developed as electrode materials for supercapacitors. The electrode materials of the cheaper transition metal oxides exhibit remarkable capacitive nature, delivering a considerable SC. However, the resistivity and the equivalent series resistance (ESR) of these cheaper transition metal oxides are very large, which greatly limits their capacity and power density available.

On the other hand, it is reported that mixed oxide composites exhibit superior capacitive performance to single transition metal oxides. It has been demonstrated that the incorporation of Ni [19], Pb [20], Mo [22], and V [23] oxides into pristine manganese oxide can enhance specific capacitance and electrical conductivity of pristine manganese oxide. Nevertheless, the effect of Co oxide addition into pristine manganese oxide has not been extensively studied yet, and the results from different research groups vary significantly [24-26].

In this work, a mesoporous Mn-Co oxide was derived from a mixed $Mn_{0.8}Co_{0.2}C_2O_4 \cdot nH_2O$, which was synthesized by a solid-state coordination reaction. Its phase compositions and microstructures were characterized by X-ray diffraction (XRD), scanning electron microscope (SEM) and N_2 adsorption-desorption measurements, and

---

[*]Corresponding author.

its electrochemical properties were analyzed by cyclic voltammetry and galvanostatic charge/discharge cycling. Considering the considerable content of cobalt added in the prepared Mn-Co oxides, and a remarkable pseudocapacitive behavior of cobalt oxide in alkaline aqueous electrolyte [17,18], KOH aqueous electrolyte was used to investigate the electrochemical properties of the Mn-Co oxide. The obtained Mn-Co oxide shows excellent capacitive performance in terms of specific capacitance (SC), power capability and cycling stability, which is promising for supercapacitor applications.

2. Experimental

2.1. Synthesis of the Mn-Co Oxide Powder

Analytical-grade manganese acetate $Mn(CH_3COO)_2 \cdot 4H_2O$, cobalt acetate $Co(CH_3COO)_2 \cdot 4H_2O$, and oxalic acid $H_2C_2O_4 \cdot 2H_2O$ were used as starting materials. All the reagents were purchased from Sinopharm Group Chemical Reagent Company in China, and used as received. A proper amount of the starting materials was weighed accurately with a molar ratio of $Mn(CH_3COO)_2 \cdot 4H_2O$:Co-$(CH_3COO)_2 \cdot 4H_2O$:$H_2C_2O_4 \cdot 2H_2O$ of 0.8:0.2:1.1, then mixed and milled in a mortar to form a powder mixture. Subsequently, the obtained powder mixture was ball milled at room temperature for 5 h in a polyethylene container using zirconia balls as milling medium. The milled mixture was dried at 80°C, resulting in a Mn-Co oxalate precursor. Finally, the Mn-Co oxalate precursor was calcined in air at 250°C for 10 h to obtimed Mn-Co oxide.

2.2. Structural Characterization

A Philips X'pert Pro X-ray diffractometer with CuK_α radiation (λ = 1.5406 Å) was used to analyze the phase compositions of the dried milled mixture and the calcined Mn-Co oxide. Diffraction data were collected in the 2θ range from 15° to 80°, using the step-scan mode with a scanning speed of 0.02° step-size and 1 s per step. The morphology of the obtained Mn-Co oxide was observed by using a JSM 6490 scanning electron microscope (SEM). N_2 adsorption-desorption measurements were carried out at a Coulter SA 3100 system at 77.3 K. The surface area was calculated using the Brunauer-Emmett-Teller (BET) equation. Pore size distributions were calculated by the Barrett-Joyner-Halenda (BJH) method. Samples were dried and degassed for 2 h at 150°C to remove any surface organic or moisture contaminants.

2.3. Electrochemical Characterization

The electrodes for electrochemical measurements consisted of the prepared Mn-Co oxide, acetylene black (AB) and polytetrafluoroethylene (PTFE), whose weight ratio was 75:20:5. First, the Mn-Co oxide and the acetylene black were fully mixed and ground, then a proper amount of PTFE binder was added into the powder mixture to achieve a homogenous slurry, followed by painting the prepared slurry onto a nickel foam current collector with an area of 1 cm × 1 cm. Finally, the painted current collector was dried for 10 h at 80°C, and pressed at a pressure of 10 MPa to form a reliable electrode. Each of the fabricated electrodes contained ~4 mg of the Mn-Co oxide electroactive material.

All the electrochemical measurements concerned were carried out in 6 mol·L^{-1} KOH aqueous electrolyte. Cyclic voltammetric measurements were performed on a CHI6-04C electrochemical workstation in a three-electrode cell set-up, using a Mn-Co oxide electrode as the working electrode, a platinum foil as the counter electrode, a saturated calomel electrode (SCE) as the reference electrode. Cyclic voltammograms at various scan rates were recorded between −0.4 and 0.4 V vs. SCE.

For evaluation of galvanostatic charge/discharge performance of the obtained Mn-Co oxide electrodes, a symmetrical capacitor was assembled using a couple of the identical electrodes separated by a porous polypropylene separator. The galvanostatic charge/discharge performance at different current densities was determined by a battery test system of Neware BTS-3008W in a potential range from 0 to 0.8 V.

3. Results and Discussion

3.1. Phase Compositions and Microstructures

Figure 1(a) gives the XRD pattern of the Mn-Co oxalate synthesized by a solid-state coordination reaction. The XRD pattern of the synthesized Mn-Co oxalate matches that of α-form manganese oxalate (JCPDS, No. 25-0544), suggesting that the synthesized oxalate is a binary Mn-Co mixed oxalate [27]. Considering a molar ratio of Mn^{2+}:Co^{2+} of 4:1 in the mixture of the starting materials used, and almost no loss of metal ions during ball-milling, the obtained Mn-Co oxalate can be expressed as a chemical formula of $Mn_{0.8}Co_{0.2}C_2O_4 \cdot nH_2O$. **Figure 1(b)** shows the
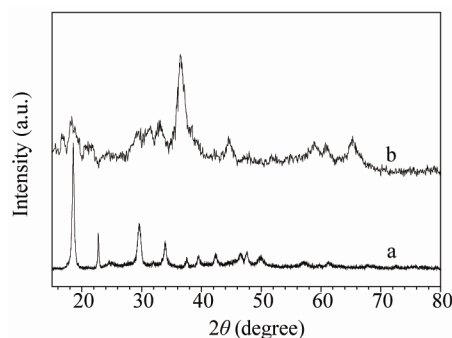

Figure 1. XRD patterns of (a) the Mn-Co oxalate and (b) the obtained Mn-Co oxide.

XRD pattern of the Mn-Co oxide powder. No characteristic diffraction peaks of the Mn-Co oxalate are observed in the XRD patttern of the calcined Mn-Co oxide in **Figure 1(b)**, indicating that thermal decomposition of the Mn-Co oxalate is nearly completed in air at 250°C in the duration of 10 h. The low intensity and remarkable broadening of the diffraction peaks disclose that the obtained Mn-Co oxide is poorly crystallized. The discernible peaks around $2\theta = 18.2°, 29.3°, 31.4°, 32.9°, 36.5°, 44.6°, 58.9°, 60.3°$ and $65.3°$ are well in accordance with those of tetragonal spinel Mn_3O_4 (JCPDS, No. 89-4837). Nevertheless, compared with the tetragonal spinel Mn_3O_4, the positions of the diffraction peaks for Mn-Co oxide shift positively, indicating the smaller lattice parameters of the obtained Mn-Co oxide. It has been demonstrated that the length of the Co^{n+}-O bond is smaller than that of the Mn^{n+}-O bond in the identical sublattice of a spinel-structured mixed oxide [28]. The smaller lattice parameters of the obtained Mn-Co oxide imply that the Co cations are incorporated into the crystal lattice of the tetragonal spinel Mn_3O_4, forming a single-phase Mn-Co mixed oxide. Therefore, the chemical formula of the obtained spinel Mn-Co oxide can be denoted as $Mn_{2.4}Co_{0.6}O_4$. Formation of the spinel Mn-Co oxide at a low calcination temperature of 250°C is probably related to the compositional homogeneity of the synthesized Mn-Co mixed oxalate [27].

Figure 2 shows the SEM images of the obtained Mn-Co oxide powder under different magnification. As seen from the lower-magnification SEM image in **Figure 2(a)**,
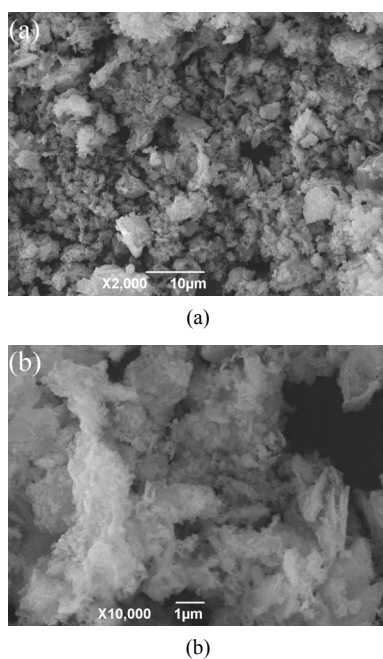
the obtained Mn-Co oxide powder is composed of irregular-shaped agglomerates with a size less than 5 μm. The higher-magnification SEM image in **Figure 2(b)** shows that each of the irregular agglomerates observed under lower magnification actually contains a great number of ultrafine primary particles with a particle size less than 100 nm. The ultra-fine particles of the prepared Mn-Co oxide certainly lead to a larger surface area available for charge storage, which is beneficial to en hancing its supercapacitive performance.

The mesoporosity and textural properties of the as-prepared Mn-Co oxide was investigated by N_2 adsorption-desorption measurement at liquid N_2 temperature. **Figure 3** gives the N_2 adsorption-desorption isotherm and BJH pore-size distribution of the Mn-Co oxide. It can be seen that the isotherm presents a typical type IV sorption behavior, indicating a mesoporous structure of the obtained Mn-Co oxide according to the classification of IUPAC [29]. Furthermore, there is an abrupt increase in adsorption volume of adsorbed N_2 at a certain P/P_0 value of 0.52. The sharp increase is generally attributed to capillary condensation, and the P/P_0 position of the inflection is associated with the pore size [30]. The BJH pore-size distribution, as given in the inset of **Figure 3**, reveals that the pore size distribution for the Mn-Co oxide is narrow and situated in the mesoporous region (2 - 50 nm). Also the textural properties of the Mn-Co oxide are given in **Table 1**. This demonstrates that the synthesis route of the solid-state coordination reaction we adopted allows the obtained Mn-Co oxide with a mesoporous structure and a considerable BET surface area, which are the desired textural properties for high-performance supercapacitor materials.
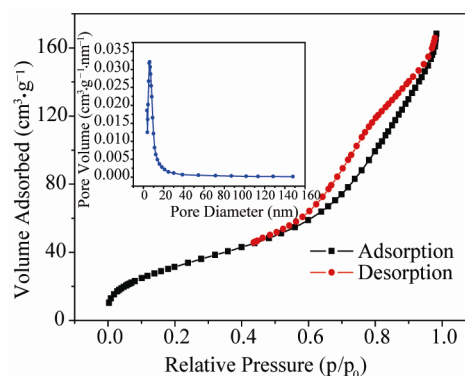

(a)

(b)

Figure 2. SEM images of the Mn-Co oxide powder under (a) lower and (b) higher magnification.

Figure 3. N_2 adsorption-desorption isotherm and BJH pore-size distribution of the as-prepared Mn-Co oxide.

Table 1. Textural properties of the as-prepared Mn-Co oxide from N_2 adsorption-desorption measurements.

BET surface ($m^2 \cdot g^{-1}$)	Pore volume ($cm^3 \cdot g^{-1}$)	Average pore size (nm)
120	0.26	19

3.2. Cyclic Voltammograms

Cyclic voltammetry is considered to be a powerful tool to indicate the capacitive behavior of electrode materials. **Figure 4** shows the cyclic voltammograms of the Mn-Co oxide electrode measured in a scan rate range from 2 to 50 mV·s^{-1} between −0.4 and 0.4 V vs. SCE in 6 mol·L^{-1} KOH aqueous electrolyte. Though slightly distorted at higher scan rates, all the cyclic voltammograms obtained are roughly rectangular in shape, and approximately symmetrical in anodic and cathodic directions, suggesting good capacitive behavior of the Mn-Co oxide electrode. The cyclic voltammograms exhibit a couple of approximately symmetric current peaks, *i.e.* an oxidation one around 0.16 V and a reduction one around 0.09 V, which are due to intercalation/detercalation of protons or alkaline metal cations in the Mn-Co oxide electrode in KOH aqueous electrolyte, indicating a remarkable faradic pseudocapacitance contribution [31]. The small potential difference between the anodic peak and the cathodic peak suggests the high reversibility of the Mn-Co oxide electrode.

Specific capacitance of the Mn-Co oxide electrode can be calculated from the cyclic voltammograms according to the formula

$$C_s = \frac{I}{mv} \tag{1}$$

where C_s is the specific capacitance (F·g^{-1}), m the mass (g) of the electroactive material, v the potential scan rate (V·s^{-1}), and I the even current response (A) defined by

$$I = \frac{1}{2(V_c - V_a)} \int i \, dV \tag{2}$$

(V_a and V_c represent the lowest and highest potentials (V), respectively). Specific capacitance and specific current of the Mn-Co oxide electrode at ovarious scan rates were calculated from the cyclic voltammograms, as given in **Figure 5**. **Figure 5(a)** shows that specific capacitance decreases with increasing scan rate. The maximum spe-
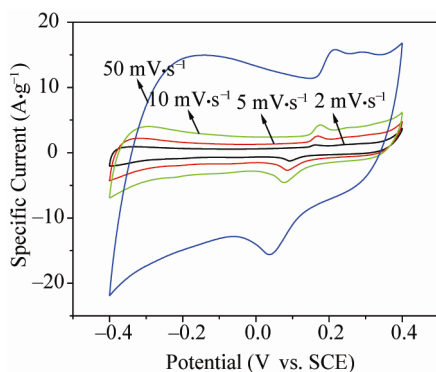
cific capacitance of 383 F·g^{-1} is obtained for the Mn-Co oxide electrode at a scan rate of 2 mV·s^{-1}. Importantly, a considerable specific capacitance of 225 F·g^{-1} is delivered even at a high scan rate of 50 mV·s^{-1}, indicating high power density of the Mn-Co oxide electrode. **Figure 5(b)** demonstrates that the specific current increases approximately linearly with increasing scan rates, confirming a high power characteristic of the Mn-Co oxide electrode material. Compared with the pristine manganese oxide consisting of α- and γ-MnO$_2$ phases derived from manganese oxalate in our previous work [32], the capacitive performance of the prepared Mn-Co oxide is much improved in the SC and power property. Notably, the specific capacitance of the obtained Mn-Co oxide electrode material is larger than that of the pristine manganese oxide electrode materials derived from sol-gel route [12], coprecipitation [33] and improved reduction reaction [34]. Moreover, the facility of the solid-state coordination reaction we adopted has the advantages of a relatively low number of processing steps, low process costs and a great convenience of obtaining mixed oxides with desired chemical compositions [35]. From a commercial and economical point of view, it is a promising method for preparation of oxide electrode materials, especially, of multi-component mixed oxide electrode materials.

3.3. Galvanostatic Charge-Discharge Analysis

A symmetrical capacitor was assembled using a couple of the identical Mn-Co oxide electrodes separated by a porous polypropylene separator. **Figure 6** shows the galvanostatic charge/discharge profiles of the Mn-Co oxide capacitor at different current densities. It can be seen that the charge/discharge profiles are somewhat curved, suggesting a pseudocapacitive characteristic of the Mn-Co oxide material. This is in accordance with the cyclic voltammetry result in **Figure 4**, where a couple of redox current peaks can be observed. The efficiency of the charge/discharge cycling is in the range of 0.88 - 0.92.
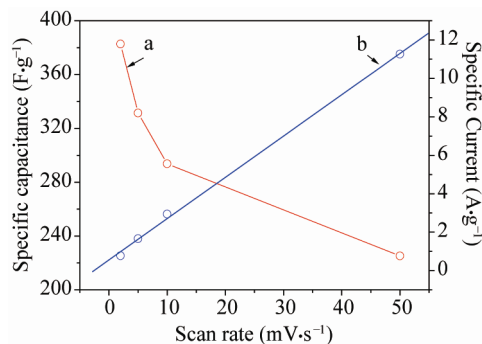

Figure 4. Cyclic voltammograms with various scan rates of the Mn-Co oxide electrode.

Figure 5. Scan rate dependence of (a) specific capacitance and (b) specific current of the obtained Mn-Co oxide electrode.

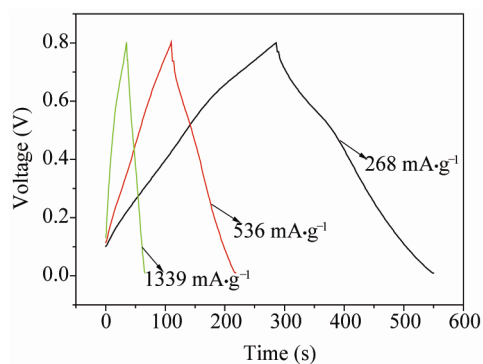**Figure 6. Galvanostatic charge/discharge profiles of the symmetrical Mn-Co oxide capacitor at various current densities.**

Figure 7. Cycling life of the symmetrical Mn-Co oxide capacitor at a current density of 1.34 A·g⁻¹ between 0 and 0.8 V.

The specific capacitance of the symmetrical Mn-Co oxide capacitor, expressed as the one of a single electrode, can be calculated by the formula, where C_s is

$$C_S = \frac{4I\Delta t}{m\Delta V} \tag{3}$$

the discharge specific capacitance (in F·g⁻¹), I the discharge current (in A), Δt the discharge time (in s), m the total mass (in g) of the electroactive material contained in the symmetrical capacitor, ΔV the discharge potential range (in V) [36]. The specific capacitance of the symmetrical Mn-Co oxide capacitor at current densities of 0.27, 0.54 and 1.34 A·g⁻¹ was calculated to be 354, 289 and 208 F·g⁻¹, respectively. Apparently, the specific capacitance reduction is relatively small when increasing current density from 0.27 to 1.34 A·g⁻¹, and a considerable specific capacitance of 208 F·g⁻¹ is still retained at a high current density of 1.34 A·g⁻¹, demonstrating a high power characteristic of the obtained Mn-Co oxide material. This is in agreement with the cyclic voltammetry result in **Figure 5(b)**, where the specific current rises almost linearly with increasing scan rates.

For examination of the long-term cycling stability of the obtained Mn-Co oxide electrode material, the symmetrical Mn-Co oxide capacitor was subjected to charge/discharge cycling at a current density of 1.34 A·g⁻¹ for consecutive 500 cycles. The variation of the specific capacitance of the capacitor with cycle number is shown in **Figure 7**. During the first 100 cycles, the specific capacitance of the capacitor fades fast, decreasing by ~12% of its initial specific capacitance. During the next 400 cycles, the specific capacitance fades slightly and becomes stable, decreasing by ~3% of its initial specific capacitance. A considerable specific capacitance of 179 F·g⁻¹, about ~85% of its initial specific capacitance, is still remained for the capacitor after 500 cycles, suggestive of good cycling stability, which is of practical importance.
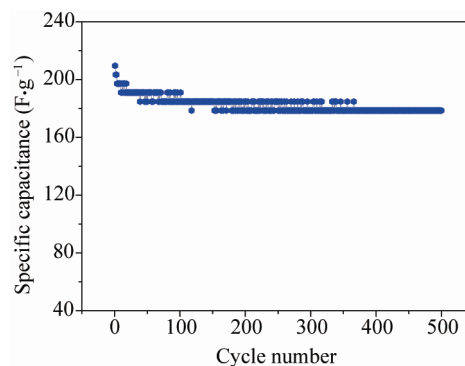
4. Conclusion

After the text edit has been completed, the paper is ready for the template. Duplicate the template file by using the Save As command, and use the naming convention prescribed by your journal for the name of your paper. In this newly created file, highlight all of the contents and import your prepared text file. You are now ready to style your paper. A mesoporous Mn-Co oxide powder with a particle size less than 100 nm was obtained by calcining the solid-state coordination reaction derived mixed oxalate $Mn_{0.8}Co_{0.2}C_2O_4 \cdot nH_2O$ in air at 250°C. The obtained Mn-Co oxide was poorly crystallized with a tetragonal spinel structure. The Mn-Co oxide electrode possesses the maximum capacitance of 383 F·g⁻¹ at a scan rate of 2 mV·s⁻¹, still retaining a considerable specific capacitance of 225 F·g⁻¹ at a high scan rate of 50 mV·s⁻¹. The specific current of the cyclic voltammograms varies roughly linearly with scan rates in the range of 2 mV·s⁻¹ to 50 mV·s⁻¹, demonstrating a high power characteristic of the obtained Mn-Co oxide electrode. At a charge/discharge current density of 1.34 A·g⁻¹, the symmetrical Mn-Co oxide capacitor exhibits a specific capacitance of 210 F·g⁻¹ during the first cycle, remaining ~85% of its initial capacitance after 500 cycles. In comparison with powder-based pristine manganese oxide material, the Mn-Co oxide material we prepared shows better supercapacitive performance, which is a promising candidate for superacpacitor materials.

5. Acknowledgements

REFERENCES

[1] B. E. Conway, "Electrochemical Supercapacitors," Kluwer Academic Publishers, New York, 1999.

MSA

[2] A. Burke, "Ultracapacitors: Why, How, and Where Is the Technology," *Journal of Power Sources*, Vol. 91, No. 1, 2000, pp. 37-50. doi:10.1016/S0378-7753(00)00485-7

[3] J. R. Miller and A. Burke, "Electrochemical Capacitors: Challenges and Opportunities for Real-World Applications," *Electrochemical Society Interface*, Vol. 17, No. 1, 2008, pp. 53-57.

[4] Y. Liu, K. X. Li, J. L. Wang, G. H. Sun and C. G. Sun, "Preparation of Spherical Activated Carbon with Hierarchical Porous Texture," *Journal of Materials Science*, Vol. 44, No. 17, 2009, pp. 4750-4753. doi:10.1007/s10853-009-3710-6

[5] A. G. Pandolfo and A. F. Hollenkamp, "Carbon Propertites and Their Role in Supercapacitors," *Journal of Power Sources*, Vol. 157, No. 1, 2006, pp. 11-27. doi:10.1016/j.jpowsour.2006.02.065

[6] T. Nathan, A. Aziz, A. F. Noor and S. R. S. Prabaharan, "Nanostructured NiO for Electrochemical Capacitors: Synthiesis and Electrochemical Properties," *Journal of Solid State Electrochemistry*, Vol. 12, No. 7-8, 2007, pp. 1003-1009. doi:10.1007/s10008-007-0465-3

[7] J. Cheng, G. P. Cao and Y. S. Yang, "Characterization of Sol-Gel-Derived NiO_x Xerogels Supercapacitors," *Journal of Power Sources*, Vol. 159, No. 1, 2006, pp. 734-731. doi:10.1016/j.jpowsour.2005.07.095

[8] D. Bélanger, T. Brousse and J. W. Long, "Manganese Oxides: Battery Materials Make the Leap to Electrochemical Capacitors," *Electrochemical Society Interface*, Vol. 17, No. 1, 2008, pp. 47-52.

[9] D. K. Bhat and M. S. Kumar, "N and P Doped Poly(3,4-Ethylenedioxythiophene) Electrode Materials for Symmetric Redox Supercapacitors," *Journal of Materials Science*, Vol. 42, No. 19, 2008, pp. 8158-8162 doi:10.1007/s10853-007-1704-9

[10] H. Guan, L. Z. Fan, H. C. Zhang and X. H. Qu, "Polyaniline Nanofiber Obtained by Interfacial Polymerization for High-Rate Supercapacitors," *Electrochimica Acta*, Vol. 56, No. 2, 2010, pp. 964-968. doi:10.1016/j.electacta.2010.09.078

[11] E. H. Liu, R. Ding, X. Y. Meng, S. T. Tan and J. C. Zhou, "Potentiodynamical Deposition of Nanosized Manganese Oxides as High Capacitance Electrochemical Capacitors," *Journal of Materials Science Materials in Electronics*, Vol. 18, No. 12, 2007, pp. 1179-1182 doi:10.1007/s10854-007-9369-3

[12] R. N. Reddy and R. G. Reddy, "Synthesis and Electrochemical Characterization of Amorphous MnO_2 Electrochemical Capacitor Electrode Material," *Journal of Power Sources*, Vol. 132, No. 1-2, 2004, pp. 315-320 doi:10.1016/j.jpowsour.2003.12.054

[13] T. Brousse, M. Toupin, R. Dugas, L. Athouël, O. Crosnier and D. Bélange, "Crystalline MnO_2 as Possible Alternatives to Amorphous Compounds in Electrochemical Supercapacitors," *Journal of the Electrochemical Society*, Vol. 153, No. 12, 2006, pp. A2171-A2180. doi:10.1149/1.2352197

[14] L. Athouel, F. Moser, R. Dugas, O. Crosnier, D. Bélanger and T. Brousse, "Variation of the MnO_2 Birnessite Structure upon Charge/Discharge in an Electrochemical Su-

[15] percapacitor Electrode in Aqueous Na_2SO_4 Electrolyte," *Journal of Physical Chemistry*, Vol. 112, No. 18, 2008, pp. 7270-7277. doi:10.1021/jp0773029

[15] F. B. Zhang, Y. K. Zhou and H. L. Li, "Nanocrystalline NiO as an Electrode Material for Electrochemical Capacitor," *Materials Chemistry and Physics*, Vol. 83, No. 2-3, 2004, pp. 260-264. doi:10.1016/j.matchemphys.2003.09.046

[16] X. M. Liu, X. G. Zhang and S. Y. Fu, "Preparation of Urchinlike NiO Nanostructures and Their Electrochemical Capacitive Behaviors," *Materials Research Bulletin*, Vol. 41, No. 3, 2006, pp. 620-627. doi:10.1016/j.materresbull.2005.09.006

[17] T. Y. Wei, C. H. Chen, K. H. Chang, S. Y. Lu and C. C. Hu, "Cobalt Oxide Aerogels of Ideal Supercapacitive Properties Prepared with an Epoxide Synthetic Route," *Chemistry of Materials*, Vol. 21, No. 14, 2009, pp. 3228-3233. doi:10.1021/cm9007365

[18] Y. Y. Gao, S. L. Chen, D. X. Cao, G. L. Wang and J. L. Yin, "Electrochemical Capacitance of Co_3O_4 Nanowire Arrays Supported on Nickel Foam," *Journal of Power Sources*, Vol. 195, No. 6, 2010, pp. 1757-1760. doi:10.1016/j.jpowsour.2009.09.048

[19] E. H. Liu, W. Li, J. Li, X. Y. Meng and S. T. Tan, "Preparation and Characterization of Nanostructured NiO/MnO_2 Composite Electrode for Electrochemical Supercapacitors," *Materials Research Bulletin*, Vol. 44, No. 5, 2009, pp. 1122-1126. doi:10.1016/j.materresbull.2008.10.003

[20] H. Kim and B. N. Popov, "Synthesis and Characterization of MnO_2 Based Mixed Oxides as Supercapacitors," *Journal of The Electrochemical Society*, Vol. 150, No. 3, 2003, pp. D56-D62. doi:10.1149/1.1541675

[21] J. P. Zheng, "Ruthenium Oxide-Carbon Composite Electrodes for Electrochemical Capacitors," *Electrochemical and Solid-State Letters*, Vol. 2, No. 8, 1999, pp. 359-361 doi:10.1149/1.1390837

[22] M. Nakayama, A. Tanaka, Y. Sato, T. Tonosaki and K. Ogura, "Electrodeposition of Manganese and Molybdenum Mixed Oxide Thin Films and Their Charge Storage Properties," *Langmuir*, Vol. 21, No. 13, 2005, pp. 5907-5913. doi:10.1021/la050114u

[23] X. Y. Xie, W. W. Liu, L. Y. Zhao and C. D. Huang, "Structural and Electrochemical Behavior of Mn-V Oxide Synthesized by a Novel Precipitation Method," *Journal of Solid State Electrochemistry*, Vol. 14, No. 1, 2010, pp. 1585-1594. doi:10.1007/s10008-009-0987-y

[24] P. Y. Chuang and C. C. Hu, "The Electrochemical Characteristics of Binary Manganese-Cobalt Oxides Prepared by Anodic Deposition," *Materials Chemistry and Physics*, Vol. 92, No. 1, 2005, pp. 138-145. doi:10.1016/j.matchemphys.2005.01.004

[25] G. Y. Zhao, C. L. Xu and H. L. Li, "Highly Ordered Cobalt-Manganese Oxide (CMO) Nanowire Array Thin Film on Ti/Si Substrate as an Electrode for Electrochemical Capacitor," *Journal of Power Sources*, Vol. 163, No. 2, 2007, pp. 1132-1136. doi:10.1016/j.jpowsour.2006.09.085

[26] E. Machefauxa, T. Brousseb, D. Bélangerc and D. Guyomard, "Supercapacitor Behavior of New Substituted Man-

ganese Dioxides," *Journal of Power Sources*, Vol. 165, No. 2, 2007, pp. 651-655 doi:10.1016/j.jpowsour.2006.10.060

[27] D. L. Fang, Z. B. Wang, P. H. Yang, W. Liu and C. S. Chen, "Preparation of Ultra-Fine Nickel Manganite Powders and Ceramics by a Solid-State Coordination Reaction," *Journal of the American Ceramic Society*, Vol. 89, No. 1, 2006, pp. 230-235. doi:10.1111/j.1551-2916.2005.00666.x

[28] D. L Fang, C. S Chena and A. J. A. Winnubstc, "Preparation and Electrical Properties of $Fe_xCu_{0.10}Ni_{0.66}Mn_{2.24-x}O_4$ $(0 \leq x \leq 0.90)$ NTC Ceramics," *Journal of Alloys and Compounds*, Vol. 454, No. 1-2, 2008, pp. 286-291. doi:10.1016/j.jallcom.2006.12.059

[29] F. Rouquerol, J. Rouquerol and K. Sing, "Adsorption by Powers and Porous Solids: Principles Methodology and Applications," Academic Press, San Diego, 1999.

[30] T. Sreethawong, S. Chavadej, S. Ngamsinlapasathian and S. Yoshikawa, "A Modified Sol-Gel Process-Derived Highly Nanocrystalline Mesoporous NiO with Narrow Pore Size Distribution," *Colloids and Surfaces A*: *Physicochemical and Engineering Aspects*, Vol. 296, No. 1-3, 2007, pp. 222-229. doi:10.1016/j.colsurfa.2006.09.048

[31] E. Raymundo-Pinero, V. Khomenko and E. Frackowiak, "Performance of Manganese Oxide/CNTs Composites as Electrode Materials for Electrochemical Capacitors," *Journal of The Electrochemical Society*, Vol. 152, No. 1, 2005, pp. 229-235. doi:10.1149/1.1834913

[32] D. L. Fang, B. C. Wu, A. Q. Mao, Y. Yan and C. H. Zheng, "Supercapacitive Properties of Ultra-Fine MnO_2 Prepared by a Solid-State Coordination Reaction," *Journal of Alloys and Compounds*, Vol. 507, No. 2, 2010, pp. 526-530. doi:10.1016/j.jallcom.2010.08.010

[33] M. Toupin, T. Brousse and D. Bélanger, "The Influence of Microstructure on the Charge Storage Properties of Chemically Synthesized Manganese Dioxide," *Chemistry of Materials*, Vol. 14, No. 9, 2002, pp. 3946-3952. doi:10.1021/cm020408q

[34] S. J. Bao, B. L. He, Y. Y. Liang, W. J. Zhou and H. L. Li, "Synthesis and Electrochemical Characterization of Amorphous MnO_2 for Electrochemical Capacitor," *Materials Science and Engineering*: *A*, Vol. 397, No. 1-2, 2005, pp. 305-309. doi:10.1016/j.msea.2005.02.058

[35] C. H. Zheng and D. L. Fang, "Preparation of Ultra-Fine Cobalt-Nickel Manganite Powders and Ceramics Derived From Mixed Oxalate," *Materials Research Bulletin*, Vol. 43, No. 7, 2008, pp. 1877-1882. doi:10.1016/j.materresbull.2007.06.061

[36] J. Li, X. Y. Wang, Q. H. Huang, S. Gamboa and P. J. Sebastian, "A New Type of $MnO_2·xH_2O$/CRF Composite Electrode for Supercapacitors," *Journal of Power Sources*, Vol. 160, No. 2, 2006, pp. 1501-1505. doi:10.1016/j.jpowsour.2006.02.045